

Review Article

Differential diagnosis and clinicopathological study of single index IVIM, DWI, and DKI models in benign and malignant breast lesions

Huiyang Wang^{1,2*}, Wenxiu Ding^{1,2*}, Xisong Zhu²

¹The 2nd Clinical Medical College, Zhejiang Chinese Medical University, No.548 Binwen Road, Binjiang District, Hangzhou 310053, Zhejiang Province, China; ²Department of Radiology, Quzhou Central Hospital Affiliated to Zhejiang Chinese Medical University, No.2 Zhonglou Bottom, Kecheng District, Quzhou 324000, Zhejiang Province, China. *Co-first authors.

Received April 28, 2020; Accepted June 26, 2020; Epub September 15, 2020; Published September 30, 2020

Abstract: Objective: To explore the value of intravoxel incoherent motion (IVIM)-diffusion-weighted imaging (DWI) and diffusion kurtosis imaging (DKI) in diagnosing benign and malignant (B/M) breast lesions (BLES), and to provide a basis for early clinical diagnosis of breast cancer (BRCA). Methods: From January 2019 to July 2019, 89 BLES patients with 96 nodules in total, were included and examined by magnetic resonance imaging (MRI) and Multi-b DWI before undergoing operation in our hospital. The apparent diffusion coefficient (ADC) was computed by the single exponential model b of 0 and 1000 s/mm², and the parameters were computed by using IVIM and DKI. One-way Analysis of Variance (ANOVA) was utilized to compare the differences of parameters in normal breast tissue (NBT) and B/M BLES. Results: 1. There were statistically significant differences in histology, signal enhancement characteristics, tic curve, maximum enhancement slope, and peak time between BRCA and benign BRCA ($P < 0.05$). 2. The values of F, D, and D* between malignant and benign BRCA were significantly different ($P < 0.05$). 3. In the IVIM model, with an increase in B value, the NBTs were determined as normal in DKI model; compared to benign BLES and NBTs, the MK value of malignant BLES was higher; meanwhile, compared to NBTs, the D* value of malignant BLES was significantly higher. Conclusion: The quantitative parameters of dynamic contrast-enhanced (DCE)-MRI and IVIM reflect the permeability and perfusion characteristics of tumor blood vessels, as well as the micro movement of water molecules in the tumor, which are more accurate for the evaluation of tumor angiogenesis and internal tissue characteristics. The D value has high diagnostic efficiency and is critical in the differential diagnosis of B/M BLES.

Keywords: DWI, IVIM, diffusion kurtosis imaging, benign and malignant breast lesions, differential diagnosis

Introduction

In recent years, due to the improvement of living standards and changes in fertility policies, the incidence rate of breast cancer (BRCA) among women in China has raised annually, which has seriously jeopardized the life and health of women. Globally, 12.2% of newly diagnosed BRCA cases occur in China, and the fatal cases of BRCA in China account for 9.6% of all BRCA deaths. At present, the incidence of BRCA among Chinese women is the highest. In China, the general age-standardized rate (ASR) is 21.6 per 100,000 women; meanwhile, the ASR (34.3 cases per 100,000 women) in urban areas is about twice that in rural areas (17.0 cases per 100,000 women) [1]. The World Health Or-

ganization (WHO) has pointed out that the early detection, diagnosis, and treatment of BRCA can reduce the mortality rate while significantly improving the prognosis of patients. Therefore, an effective diagnosis of early BRCA is very important for the prognosis of patients. However, compared with the developed countries, the onset age of BRCA among Chinese women is decreasing, and the screening rate is also lower. Many severe cases are consequences of delayed diagnosis; at the time of diagnosis, the patients are already in advanced stage, which leads to poor treatment and even deaths [2].

Early stage and identified BRCA is considered to be a potentially curable disease; therefore, the differential diagnosis of benign and malig-

nant (B/M) BRCA is vital in determining the treatment plans and improving the therapeutic effects [3]. In general, benign breast masses are mostly oval, with rounded density increase. The border is smooth and sharp. Benign breast masses are often a single mass, while that of the fibroadenomas can be multiple masses. There are also relatively dense benign tumors, such as wrapped hematoma, hamartoma, and lipid cysts. However, a few malignant tumors are also elliptical in shape, with smooth and sharp edges, such as simple cancer or medullary carcinoma, which are easily misdiagnosed as benign lesions. Malignant tumors are often lobulated, star-shaped, or burr-like, which is caused by the infiltration and growth in the surrounding tissues. At present, for the early diagnosis of breast malignant tumors, medical imaging examinations are critical, including mammography, breast ultrasonography, and breast magnetic resonance imaging (MRI) [4]. Mammography is easy in operation and economical; therefore, it is widely utilized in BRCA screening. However, for diagnosing small and deep lesions, especially dense breast lesion (BLES), the diagnostic advantages of breast MRI are more obvious.

At present, with the continuous development of magnetic resonance technology, mammography dynamic contrast-enhanced MRI (DCE-MRI) and diffusion-weighted imaging (DWI) have gradually evolved from the most primitive routine imaging examinations based on anatomical changes into multi-functional MRI examination techniques for detecting various micro-environments, such as tissue components and blood perfusion [5-7]. DWI can quantitatively detect the microscopic Brownian motion of water molecules in living tissues; therefore, the pathological changes in the body tissue cells can be found to improve the benign and malignant specificity of DCE-MRI in diagnosing BLES. However, the apparent diffusion coefficient (ADC) values measured by the traditional DWI single-index model are susceptible to micro-perfusion factors; especially, the blood supply of malignant tumors is more abundant, and the error of ADC values is greater [8-11]. The double exponential model of intravoxel incoherent motion (IVIM) can distinguish diffusion and perfusion in tissues and avoid the interference of perfusion factors on ADC values, which is effective in the differential diagnosis of B/M BLES. Therefore, the diagnostic values of IVIM-DWI and diffusion kurtosis imaging (DKI) for B/M BLES are explored by ana-

lyzing the imaging data of patients with breast tumors.

Materials and methods

Objects of study

From January 2019 to July 2019, 89 BLES patients with 96 nodules in total, who were examined by MRI and Multi-b DWI before the operation in Quzhou Central Hospital Affiliated to Zhejiang Chinese Medical University, were prospectively included. All the patients were female, and sought medical help due to breast masses. Exclusion criteria: (1) measurement and interpretation of data were affected due to DWI image artifacts; (2) lower signal intensity in upper lesions in DWI images; (3) lesion diameter < 8 mm; (4) DCE-MRI and the region of interest (ROI) cannot be obtained. According to the above criteria, the pathological results of 81 patients were obtained, with a total of 88 lesions, in which 31 cases were benign BLES and 55 were breast malignant lesions. The patients were 23 to 78 years old and the average age was (48.14±13.98). All patients underwent pathological biopsy, surgery, radiotherapy, and chemotherapy before MRI, and were treated within 10 days after the examination. All lesions were confirmed by surgical pathology or biopsy. This experiment was approved by the ethics committee of Quzhou Central Hospital Affiliated to Zhejiang Chinese Medical University and was in accordance with the Helsinki Declaration. All the patients and their families were aware of the experimental content and signed the informed consent forms.

Among all the enrolled patients, 28 were benign cases, 3 of which had 2 lesions, and there were 31 benign lesions in total; meanwhile, 53 were malignant cases, 4 of which had 2 lesions, and there were 57 malignant lesions in total. Among all the benign lesions, there were 12 cases of breast fibroids, 10 breast granuloma, and 9 breast diseases. Among all the malignant lesions, there were 37 cases of invasive ductal carcinomas (19 were grade II differentiation and 17 were grade III differentiation), 11 ductal carcinomas in situ, 3 papilloma, 3 mucinous adenomas, 1 lymphoma, and 1 borderline lobular tumor.

Examination methods

Before the examination, patients with cardiac pacemakers, surgical implants, and adverse

reactions to gadolinium contrast agents in previous MRI examinations were excluded. Any ferromagnetic metal must be removed before the examination. The patient to be examined was told to wear comfortable and convenient clothes, and the bodyweight was measured accurately. The patient lied protractedly on the examination bed, with her feet towards the entrance of the MRI scanner. Given the precondition of feeling comfortable or tolerable, the patient's arms were at both sides of her head, and her breasts naturally sagged at the specific positions of the breast coils. The patient was told to breathe evenly to reduce artifacts caused by sharp chest movements.

(1) Scanning equipment and position: a 1.5T (Siemens MAGNETOM Aera) superconducting MRI magnetic resonance scanner was used, an 8-channel breast dedicated phased array coil was utilized as the receiving coil. The axial T1 weighted images, axial pressure fattened T2 weighted images, multiple b value diffusion weighted imaging (IVIM), and DCE-MRI enhanced scans were performed in sequence.

(2) Routine scans: the routine scans included localized scans of the horizontal, sagittal, and coronal positions of the breast. The fast inversion recovery magnetization was used to prepare the spin-echo pressure T2WI sequence (TR=5600 ms, TE=65 ms, TI=170 ms, FOV=340 mm × 340 mm) and the small-angle excitation three-dimensional imaging (FLASH-3D) T1WI sequence (TR=8.5 ms, TE=4.74 ms, slice thickness=4.0 mm, FA=20°) for the cross-sectional scanning. Besides, the automated calibration and data acquisition were performed by GRAPPA technology.

Multi-b value dispersion weighted imaging (IVIM): a single-shot echo-planar imaging sequence was applied simultaneously in three directions of x, y, and z for diffusion-weighted signal acquisition. The b values took 0, 50, 100, 150, 200, 250, 400, 600, 800, and 1000 s/mm², TR/TE=4200 ms/70 ms, slice thickness was 4.0 mm, slice spacing was 1.0 mm, the matrix was 160 × 128, and the excitation times were 5.

Performing high-b value dispersion-weighted imaging (DKI): a single-shot echo planar imaging sequence was used. The b values took 0, 600, 1200, and 2400 s/mm², TR/TE=6200 ms/100 ms, slice thickness was 4.0 mm, slice

spacing was 1.0 mm, the matrix was 160 × 128, and excitation times were 3.

(3) DCE-MRI scans: the FLASH-3D pressure-preserved T1WI sequence was used, TR=4.50 ms, TE=1.55 ms, slice thickness was 3.0 mm, slice spacing was 0, with a total of 80 slices; FA=10°, FOV was 340 mm × 340 mm, the matrix was 320 × 430; each scan lasted 30 s and was repeated 8 times. Venous access before the DCE-MRI examination was established for each patient, with gadopentetate (manufacturer: Shanghai Xinhualian Pharmaceutical, China; certificate number: Guoyao Zhunzi H19991080) as a contrast agent, which was given at a dosage of 0.2 mL/kg and a rate of 0.2 mL/s. The system would automatically generate an enhanced image and a maximum signal intensity projection image.

Image analysis and processing

To reduce the measurement errors due to ROI selection bias, all measurements were repeated thrice and averaged. The conventional MRI images were sent to the Siemens Syngo software system for analysis and evaluation. Two doctors from the oncology department and the radiology department jointly read the images, and the lesions were described as masses or non-masses according to the MRI standardized language standard (ACR BI-RADS-MRI). For the mass-enhanced lesions, the time-signal intensity curve (TIC) was drawn by using the Mean Curve software. The region with high signal dispersion and the most obvious enhancement was selected as the ROI. The ROI should be within the contour of the lesion, with an area of 15~210 mm² and an average of 68 mm² while avoiding the selection of central necrosis, hemorrhage, cystic alterations, and surrounding normal tissue or adipose tissue. In the case of selecting ROI for non-mass-enhanced lesions, the area with a high signal on the DWI and the most obvious enhancement was selected [12].

The dynamic enhanced scan sequence images were sent to the Syngo MMWP workstation to have the specific morphology and signal enhancement characteristics of the lesion sites observed. The most obvious physical part of the lesion enhancement was selected as the ROI area of 5~9.5 mm² in addition to the site of necrosis, hemorrhage, and cystic change. The TIC curve was drawn by using the Mean Curve software and calculated according to the signal

Table 1. The comparison of DCE-MRI examination indicators of B/M BLES

Tumor properties	Form		Strengthening characteristics		TTP	MSI	TIC type	
	Rule	Irregularity	Even	Uneven	Median	Median	Continuous rising	Platform and continuous descent
Benign	8 (25.8%)	23 (74.2%)	20 (64.5%)	11 (35.5%)	194.52	2.08	20 (64.5%)	11 (35.5%)
Malignant	44 (77.2%)*	13 (22.8%)*	18 (31.6%)	39 (68.4%)	128.36*	2.77*	12 (21.1%)*	45 (78.9%)*
P	< 0.001		0.079		< 0.001	0.030	< 0.001	

*Compared with Benign group, P < 0.05.

intensity peak time (TTP). The maximum slope (MSI) was derived [13].

The ADC was automatically produced by a single exponential model with b values of 0 and 1000 s/mm². The segmentation double-index IVIM model was utilized to determine the diffusion coefficient (D value) of pure water molecules, the pseudo-diffusion coefficient (D* value) generated by micro-circulation perfusion, and the proportion of micro-circulation perfusion tissue diffusion, i.e., the perfusion fraction (f-value) and blood flow (BF). The DKI model was used to calculate the diffuse kurtosis (MK) and the average dispersion (MD). The upper limit of the b value for generating the D* value pseudo color parameter map was set to 200 s/mm². The ROI of the dynamic contrast-enhanced image was taken as a reference to select the ROI containing most of the lesions as much as possible, and the size of ROI was 55-200 mm².

Statistical methods

The SPSS 20.0 statistics software package was applied for statistical analysis of the data. The normal distribution test was performed on the quantitative data such as the DCE-MRI examination of the B/M BLES and the quantitative parameters of the IVIM-DWI examination. The results consistent with the normal distribution were written as mean number \pm standard deviation. First, the single-sample Levene's variance homogeneity test was performed. All patients were grouped according to benign lesions and malignant lesions. The D, f, D*, MK, MD and ADC values of each group were compared with the normal control group. The one-way Analysis of Variance (ANOVA) was utilized to compare the differences of groups. The receiver operating characteristic curve (ROC) was drawn, the area under the curve (AUC) was computed, and the Z test was performed. According to the Youden index, the optimal diagnostic cut-point value of each parameter

for the evaluation of malignant tumors was found. Then, the sensitivity and specificity were further computed. The efficacy of various parameters in the differential diagnosis of B/M BLES was analyzed. If P was < 0.05, the difference indicated statistical significance.

Results

The comparison of DCE-MRI examination indicators of B/M BLES

Among the 31 benign lesions of 28 benign patients, there were 8 (25.8%) lesions with irregular tumor morphology and 23 (74.2%) lesions with circular or nearly circular shapes. There were 20 (64.5%) evenly-enhanced lesions and 11 (35.5%) unevenly-enhanced lesions. The median TTP of benign lesions was 194.52, and the median MSI was 2.08. There were 20 (64.5%) type I TIC curves and 11 (35.5%) type II/type III TIC curves. Among the 57 malignant lesions of 53 malignant patients, there were 44 (77.2%) lesions with irregular tumor morphology and 13 (22.8%) lesions with regular tumor morphology. There were 18 (31.6%) evenly enhanced lesions and 39 (68.4%) unevenly enhanced lesions. The median TTP of malignant lesions was 128.36, and the median MSI was 2.77. There were 12 (21.1%) type I TIC curves and 45 (78.9%) type II and type III TIC curves. The B/M BLES were statistically different (P < 0.05) in terms of histopathological features, signal enhancement characteristics, TIC curves, maximum enhancement slopes, and peak time. The comparison results of the DCE-MRI examination parameters of all patients were listed in **Table 1**. The comparison results of TIC curves of B/M BLES were shown in **Figure 1**.

The comparison of IVIM-DWI examination indicators of B/M BLES

Among the 31 benign lesions of 28 benign tumor patients, the average f value was 6.99%,

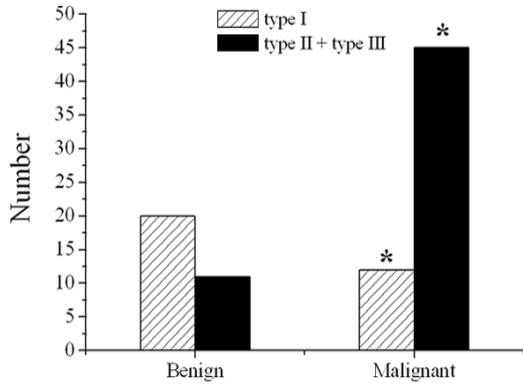


Figure 1. Comparison results of TIC curves of B/M BLES. *: Compared with Benign group, P < 0.05.

Table 2. The comparison of IVIM-DWI examination indicators of B/M BLES

Tumor properties	f (%)	D (s/mm ²)	D* (s/mm ²)
Benign	6.99	1.30 × 10 ⁻³	6.86 × 10 ⁻³
Malignant	8.18*	1.04 × 10 ^{-3*}	7.30 × 10 ^{-3*}
t	2.366	-3.976	2.120
P	< 0.05	< 0.05	< 0.05

*Compared with Benign group, P < 0.05.

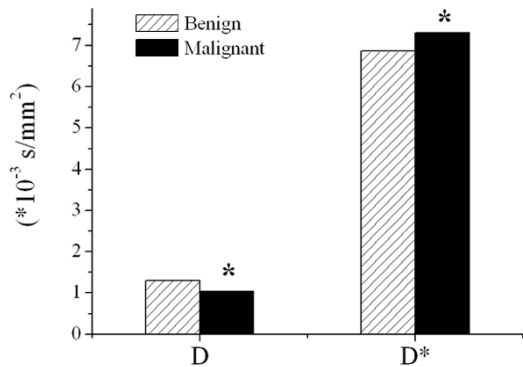


Figure 2. The comparison between D values and D* results of B/M BLES. *: Compared with Benign group, P < 0.05.

the average D value was 1.30 × 10⁻³ s/mm², and the average D* value was 6.86 × 10⁻³ s/mm². Among the 57 malignant lesions of 53 malignant patients, the average f value was 8.18%, the average D value was 1.04 × 10⁻³ s/mm², and the average D* value was 7.30 × 10⁻³ s/mm². The malignant BLES were drastically different from the benign BLES in f value, D value and D*, which had statistical significance (P < 0.05). The results of the IVIM-DWI examination parameters of all patients were com-

pared were shown in **Table 2**. The comparison of D value and D* of B/M BLES was shown in **Figure 2**.

The signal attenuation curves of BLES and NBTs

In the IVIM model, the signal attenuation curves of NBT and B/M BLES were different. With the increase in b value, the signals of NBT and B/M BLES showed the nonlinear attenuation. When the b value was < 200 s/mm², the signal of breast tissue was attenuated obviously; especially, the malignant lesions had the fastest decay rate while the benign lesions of the breast and NBT had a slower decay rate. When the b value was > 200 s/mm², the signal attenuation rate of the breast tissue gradually slowed down. When the b value was =1200 s/mm², the signal of NBT was basically attenuated. At this time, the signal of benign BLES was slightly higher; compared to benign lesions, the signal of malignant BLES was higher. In DKI model, the signal attenuation of breast tissue was a curvilinear decay, and the signal attenuation of breast malignant lesions was the fastest. The signal attenuation curves of the breast tissues of the IVIM model and the DKI model were shown in **Figures 3 and 4**, respectively.

The ADC, MD, and MK values had statistically significant differences among NBT, benign BLES, and malignant BLES (P < 0.001). Compared to benign BLES and NBT, the MK value of malignant BLES was higher, which had statistical significance (P=0.000). Compared to NBT, the D* value of malignant BLES was higher, which had statistical significance (P=0.000). The difference between parameters of benign BLES and NBT also had statistical significance (P < 0.05). Besides, in the three cases of breast tissue, the ADC values, MD values, and D values were negatively correlated to MK values. The distribution of ADC values between NBT, benign BLES, and malignant BLES was shown in **Figure 5**.

Diagnostic efficacy of DCE-MRI combined with IVIM-DWI on BLES

Of all the 31 benign BLES patients enrolled in this study, 3 were diagnosed as malignant with DCE-MRI diagnosis, and 4 were diagnosed as malignant with IVIM-DWI. However, with the joint diagnosis of DCE-MRI and IVIM-DWI, these 7 cases were accurately diagnosed as benign.

DKI with DWI, IVIM and diffusion kurtosis

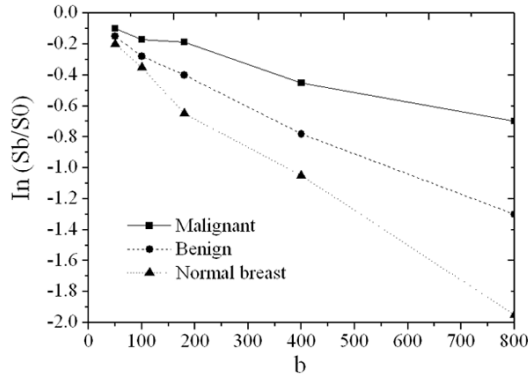


Figure 3. Attenuation curve of breast tissue signal of IVIM model.

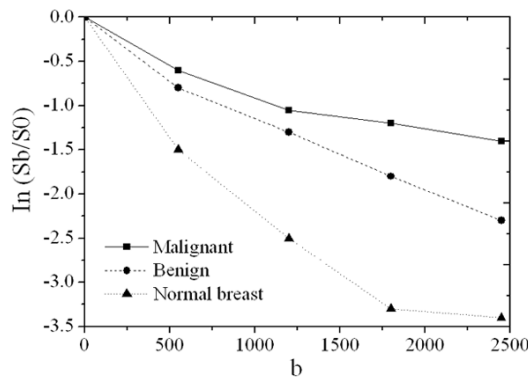


Figure 4. Attenuation curve of breast tissue signal of DKI model.

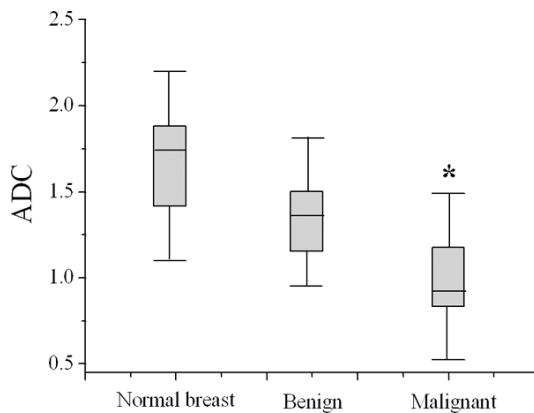


Figure 5. Attenuation curve of breast tissue signal of DKI model. *; Compared with Benign group and Normal breast, $P < 0.05$.

Therefore, a total of 3 BLES cases were diagnosed as false positive by DCE-MRI scan, IVIM-DWI scan, and the joint scan, including 1 breast fibroadenomas, 1 granulomatous mastitis, and 1 intraductal papilloma. Of all the 57 malignant

BLES cases, 12 were suspected to be malignant but not clearly diagnosed by DCE-MRI. In addition, 5 were diagnosed as benign with DCE-MRI, and 11 were diagnosed as benign with IVIM-DWI diagnosis. However, with the joint diagnosis of DCE-MRI and IVIM-DWI, these 16 BLES cases that were previously diagnosed as benign were diagnosed as malignant. Therefore, a total of 6 BLES cases were diagnosed as false-negative by DCE-MRI scan, IVIM-DWI scan, and joint scan, including 3 ductal carcinomas in situ, 2 mucinous adenomas, and 1 papilloma. The diagnostic efficacy of DCE-MRI combined with IVIM-DWI for BLES were shown in **Table 3** and **Figure 6**. The results of a 48-year-old female patient with a diagnosis of right breast fibroadenomas were analyzed. **Figure 7** showed the results of DCE-MRI in the breast, and T1WI showed a uniform low signal. **Figure 8** showed the results processed by IVIM-DWI, where the lesion was a relatively homogeneous signal and visible in the punctate signal.

Discussion

BLES is a common disease that harms the health and even the lives of women, which mainly includes mastitis lesions, breast cysts, breast fibroadenomas, and malignant BLES [14-16]. There are crossovers in the clinical manifestations of B/M BLES. Imaging technologies are currently the major method for clinically identifying B/M BLES. The incidence rate of BRCA in women in China ranks first among all malignant tumors, which keeps increasing annually. Therefore, early detection and diagnosis of BRCA are very important for the treatment and prognosis of patients. The promotion and application of breast MRI functional imaging will improve the accuracy of the differential diagnosis of B/M BLES. Clinically, breast MRI has the advantages of being multi-parameter, multi-directional, and multi-sequence imaging, which has become the most effective supplement in breast imaging examination [17, 18].

With the development of magnetic resonance technology and the wide application of computer technology, more magnetic resonance technologies with new functions have been applied to the examination of BLES [19]. DWI, as one of the common scanning sequences, is the only sequence that quantitatively detects the microscopic Brownian motion of water molecules in living tissues and quantitatively de-

Table 3. Diagnostic efficacy of DCE-MRI combined with IVIM-DWI on BLES

Inspection method	AUC	Accuracy	Susceptibility	Specificity
DCE-MRI	0.75	0.75	0.78	0.71
IVIM-DWI	0.79	0.69	0.71	0.67
DCE-MRI + IVIM-DWI	0.81*	0.82*	0.84*	0.79*

*Compared with DCE-MRI and IVIM-DWI, $P < 0.05$.

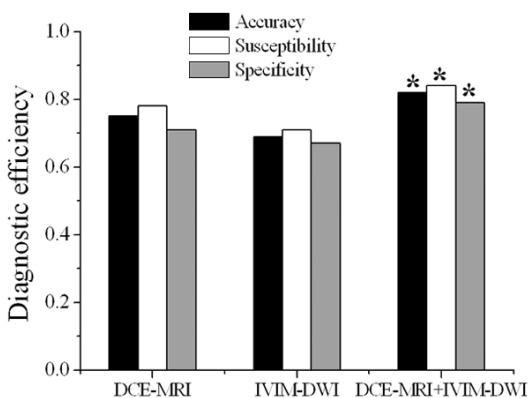


Figure 6. Comparison of the efficacy of different methods for diagnosing BLES. *; Compared with DCE-MRI and IVIM-DWI, $P < 0.05$.

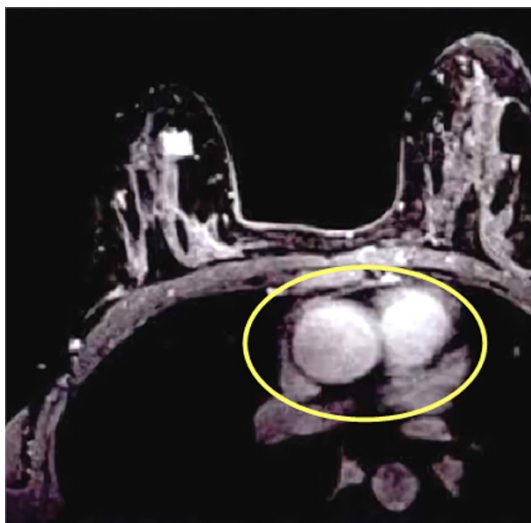


Figure 7. DCE-MRI image of breast fibroadenomas.

describes the ability of water molecules to diffuse under different b values by apparent diffusion coefficient (ADC). Indirectly, it reflects the microstructure within the organization [20]. DWI can improve the specificity of breast disease diagnosis; therefore, it is an effective supplement to MRI. DKI is a new and promising inspection technique in clinical practice. It is

based in the consideration that the microenvironment is heterogeneous and the free dispersion displacement of water molecules deviates from the Gaussian distribution [21-23]. IVIM refers to the attenuation of signals within voxels, including the diffusion of true water molecules and random blood flow microcirculation perfusion

in capillary networks. It comprehensively analyzes tissue diffusion imaging data and reveals the pathophysiological changes of diseases. In general, diffusion imaging estimates and separates tissue perfusion and diffusion effects by using multiple b-value data and IVIM models.

The dual exponential model of IVIM could distinguish diffusion and perfusion in the tissue and avoid the interference of ADC value by perfusion factors, which had accurate results in the differential diagnosis of B/M BLES. Some reports suggested that IVIM technology had higher application value in BRCA diagnosis and could improve the specificity of BRCA diagnosis by magnetic resonance technology. The D values of malignant BLES (including ductal cancer) and normal breast glandular structures had statistically significant differences. It was believed that the D value showed the effect of pure water molecule diffusion, removed the effect of vascular perfusion, and reflected cell density more accurately, which had a higher diagnostic value than ADC. Here, the diagnostic value of IVIM and DKI for B/M BLES was analyzed through the images of patients with breast diseases. The results showed that the quantitative parameters of DCE-MRI and IVIM reflected the permeability and perfusion characteristics of tumor blood vessels and the microscopic movement of water molecules inside the tumor. The evaluation of tumor angiogenesis status and internal tissue characteristics was more accurate, and the D value had higher diagnostic efficiency. Therefore, it is critical in the differential diagnosis of B/M BLES. In the IVIM model, the parameter D value was optimal for diagnosing malignant BLES. The DKI model has the highest diagnostic efficiency. MD improves the discriminating ability of the lesions. However, the data analyzed in this experiment were not compared with the morphological performances, which will be improved in the subsequent study.



Figure 8. IVIM-DWI-processed image of breast fibroadenomas.

Disclosure of conflict of interest

None.

Address correspondence to: Xisong Zhu, Department of Radiology, Quzhou Central Hospital Affiliated to Zhejiang Chinese Medical University, No.2 Zhonglou Bottom, Kecheng District, Quzhou 324-000, Zhejiang Province, China. E-mail: xisbwyocp-094011@163.com

References

- [1] Zhou S, Yi Y and Xu L. Comments on “intravoxel incoherent motion diffusion-weighted imaging as an adjunct to dynamic contrast-enhanced MRI to improve accuracy of the differential diagnosis of benign and malignant breast lesions”. *Magn Reson Imaging* 2018; 49: 161.
- [2] Chen W, Zhang J, Long D, Wang Z and Zhu JM. Optimization of intra-voxel incoherent motion measurement in diffusion-weighted imaging of breast cancer. *J Appl Clin Med Phys* 2017; 18: 191-199.
- [3] Cho GY, Gennaro L, Sutton EJ, Zabor EC, Zhang Z, Giri D, Moy L, Sodickson DK, Morris EA, Sigmund EE and Thakur SB. Intravoxel incoherent motion (IVIM) histogram biomarkers for prediction of neoadjuvant treatment response in breast cancer patients. *Eur J Radiol Open* 2017; 4: 101-107.
- [4] Li JL, Ye WT, Liu ZY, Yan LF, Luo W, Cao XM and Liang C. Comparison of microvascular perfusion evaluation among IVIM-DWI, CT perfusion imaging and histological microvessel density in rabbit liver VX2 tumors. *Magn Reson Imaging* 2018; 46: 64-69.
- [5] Pesapane F, Patella F, Fumarola EM, Panella S, Ierardi AM, Pompili GG, Franceschelli G, Ang-

- ileri SA, Magenta Biasina A and Carrafiello G. Intravoxel incoherent motion (IVIM) diffusion weighted imaging (DWI) in the periferic prostate cancer detection and stratification. *Med Oncol* 2017; 34: 35.
- [6] Ma D, Lu F, Zou X, Zhang H, Li Y, Zhang L, Chen L, Qin D and Wang B. Intravoxel incoherent motion diffusion-weighted imaging as an adjunct to dynamic contrast-enhanced MRI to improve accuracy of the differential diagnosis of benign and malignant breast lesions. *Magn Reson Imaging* 2017; 36: 175-179.
- [7] Kawashima H, Miyati T, Ohno N, Ohno M, Inokuchi M, Ikeda H and Gabata T. Differentiation between luminal-A and luminal-B breast cancer using intravoxel incoherent motion and dynamic contrast-enhanced magnetic resonance imaging. *Acad Radiol* 2017; 24: 1575.
- [8] Lee YJ, Kim SH, Kang BJ, Kang YJ, Yoo H, Yoo J, Lee J, Son YH and Grimm R. Intravoxel incoherent motion (IVIM)-derived parameters in diffusion-weighted MRI: associations with prognostic factors in invasive ductal carcinoma. *J Magn Reson Imaging* 2017; 45: 67.
- [9] Huang Y, Lin Y, Hu W, Ma C, Lin W, Wang Z, Liang J, Ye W, Zhao J and Wu R. Diffusion kurtosis at 3.0T as an in vivo imaging marker for breast cancer characterization: correlation with prognostic factors. *J Magn Reson Imaging* 2018; 49: 45.
- [10] Saadatmand S, Geuzinge HA, Rutgers EJ, Mann RM, de Roy van Zuidewijn DBW, Zonderland HM, Tollenaar RAEM, Lobbes MBI, Ausems MGEM, van 't Riet M, Hooning MJ, Mares-Engelberts I, Luiten EJ, Heijnsdijk EAM, Verhoef C, Karssemeijer N, Oosterwijk JC, Obdeijn IM, de Koning HJ and Tilanus-Linthorst MMA. MRI versus mammography for breast cancer screening in women with familial risk (FaMRIsc): a multicentre, randomised, controlled trial. *Lancet Oncol* 2019; 20: 1136.
- [11] Kataoka A, Sawaki M, Okumura S, Onishi S, Iwase M, Sugino K, Ishiguro J, Gondo N, Kotani H, Yoshimura A, Hattori M, Sasaki E, Yatabe Y, Yoshimura K, Omi K and Iwata H. Prediction of pathological margin status using preoperative contrast-enhanced MRI in patients with early breast cancer who underwent skin-sparing mastectomy. *Breast J* 2019; 25: 202-206.
- [12] Bick U, Engel C and Krug B. High-risk breast cancer surveillance with MRI: 10-year experience from the German consortium for hereditary breast and ovarian cancer. *Breast Cancer Res Treat* 2019; 175: 217-228.
- [13] Dijkstra H, Dorrius MD, Wielema M, Pijnappel RM, Oudkerk M and Sijens PE. Quantitative DWI implemented after DCE-MRI yields increased specificity for BI-RADS 3 and 4 breast lesions. *J Magn Reson Imaging* 2016; 44: 1642-1649.

DKI with DWI, IVIM and diffusion kurtosis

- [14] Cho GY, Moy L, Kim SG, Baete SH, Moccaldi M, Babb JS, Sodickson DK and Sigmund EE. Evaluation of breast cancer using intravoxel incoherent motion (IVIM) histogram analysis: comparison with malignant status, histological subtype, and molecular prognostic factors. *Eur Radiol* 2016; 26: 2547-2558.
- [15] Partridge SC and Amornsiripanitch N. The role of DWI in the assessment of breast lesions. *Top Magn Reson Imaging* 2017; 26: 201.
- [16] Liu C, Wang K, Chan Q, Liu Z, Zhang J, He H, Zhang S and Liang C. Intravoxel incoherent motion MR imaging for breast lesions: comparison and correlation with pharmacokinetic evaluation from dynamic contrast-enhanced MR imaging. *Eur Radiol* 2016; 26: 3888-3898.
- [17] Lee YJ, Kim SH, Kang BJ, Kang YJ, Yoo H, Yoo J, Lee J, Son YH and Grimm R. Intravoxel incoherent motion (IVIM)-derived parameters in diffusion-weighted MRI: associations with prognostic factors in invasive ductal carcinoma. *J Magn Reson Imaging* 2017; 45: 1394-1406.
- [18] Wei L, Chen D, Sun J, He C, Liu Y and Han D. Value of intravoxel incoherent motion model of MRI in differentiating benign from malignant breast lesions. *Chin J Med Imaging* 2016; 24: 906-908.
- [19] Wang Q, Guo Y, Zhang J, Wang Z, Huang M and Zhang Y. Contribution of IVIM to conventional dynamic contrast-enhanced and diffusion-weighted MRI in differentiating benign from malignant breast masses. *Breast Care* 2016; 11: 254-258.
- [20] Partridge SC, Nissan N, Rahbar H, Chen YQ, Yang WT, Gu YJ and Peng WJ. Diffusion-weighted breast MRI: clinical applications and emerging techniques. *J Magn Reson Imaging* 2017; 45: 337-355.
- [21] You C, Li J, Zhi W, Kühn B and Wang XL. The volumetric-tumour histogram-based analysis of intravoxel incoherent motion and non-Gaussian diffusion MRI: association with prognostic factors in HER2-positive breast cancer. *J Transl Med* 2019; 17: 182.
- [22] Wu L, Li J, Fu C, Kühn B, Wang X. Chemotherapy response of pancreatic cancer by diffusion-weighted imaging (DWI) and intravoxel incoherent motion DWI (IVIM-DWI) in an orthotopic mouse model. *MAGMA* 2019; 32: 501-509.
- [23] Tao WJ, Zhang HX, Zhang LM, Gao F, Huang W, Liu Y, Zhu Y and Bai GJ. Combined application of pharmacokinetic DCE-MRI and IVIM-DWI could improve detection efficiency in early diagnosis of ductal carcinoma in situ. *J Appl Clin Med Phys* 2019; 20: 142-150.